

Modelling the effect of shear strength on isentropic compression experiments

Stuart Thomson, Peter Howell, John Ockendon, and Hilary Ockendon

Citation: [AIP Conference Proceedings](#) **1793**, 050018 (2017); doi: 10.1063/1.4971552

View online: <http://dx.doi.org/10.1063/1.4971552>

View Table of Contents: <http://aip.scitation.org/toc/apc/1793/1>

Published by the [American Institute of Physics](#)

Articles you may be interested in

[Results from new multi-megabar shockless compression experiments at the Z machine](#)

AIP Conference Proceedings **1793**, 060015060015 (2017); 10.1063/1.4971571

[Shock compression dynamics under a microscope](#)

AIP Conference Proceedings **1793**, 020001020001 (2017); 10.1063/1.4971456

[Complete forms of Mie-Grüneisen equation of state](#)

AIP Conference Proceedings **1793**, 050001050001 (2017); 10.1063/1.4971535

[Forward modeling of shock-ramped tantalum](#)

AIP Conference Proceedings **1793**, 050021050021 (2017); 10.1063/1.4971555

[An alternative approach to Mie-Grüneisen](#)

AIP Conference Proceedings **1793**, 050002050002 (2017); 10.1063/1.4971536

[A perspective on modeling the multiscale response of energetic materials](#)

AIP Conference Proceedings **1793**, 020003020003 (2017); 10.1063/1.4971458

Modelling the Effect of Shear Strength on Isentropic Compression Experiments

Stuart Thomson^{1,a)}, Peter Howell¹, John Ockendon¹ and Hilary Ockendon¹

¹*Mathematical Institute, University of Oxford, Andrew Wiles Building, Radcliffe Observatory Quarter, Woodstock Road, Oxford, OX2 6GG*

^{a)}Corresponding author: thomson@maths.ox.ac.uk

Abstract. Isentropic compression experiments (ICE) are a way of obtaining equation of state information for metals undergoing violent plastic deformation. In a typical experiment, millimetre thick metal samples are subjected to pressures on the order of $10 - 10^2$ GPa, while the yield strength of the material can be as low as 10^{-2} GPa. The analysis of such experiments has so far neglected the effect of shear strength, instead treating the highly plasticised metal as an inviscid compressible fluid. However making this approximation belies the basic elastic nature of a solid object. A more accurate method should strive to incorporate the small but measurable effects of shear strength. Here we present a one-dimensional mathematical model for elastoplasticity at high stress which allows for both compressibility and the shear strength of the material. In the limit of zero yield stress this model reproduces the hydrodynamic models currently used to analyse ICEs. Numerical solutions of the governing equations will then be presented for problems relevant to ICEs in order to investigate the effects of shear strength compared with a model based purely on hydrodynamics.

INTRODUCTION

Under extreme conditions the ability of a solid to resist shear is limited by the yield strength of the material, which may be much smaller than the applied stress. The most rudimentary models of violent elastic-plastic deformation therefore treat the material as an inviscid compressible fluid. However, the resulting models require the specification of an *a priori* unknown equation of state (EoS). The challenge for theoreticians is to then determine this EoS using experimental evidence. A method for obtaining such information is through so-called isentropic compression experiments (ICEs); a schematic of a typical experiment is shown in Figure 1(a). Using a magnetic pressure drive, a ramped compression wave is made to propagate through the target material. Velocity interferometry (VISAR) is then used to detect the arrival of waves at the free-surface of the target sample. Figure 1(b) shows the results of a recent experiment by Rothman et al. [1] on the “Z”-machine. Here the authors subject lead samples of varying thicknesses to pressures of around 300 GPa while the yield strength can be as low as 70 MPa. When an attempt is made to reconstruct these velocity profiles numerically by tuning parameters in the constitutive assumptions of the model, the problem becomes an inverse problem for the EoS.

However, making the assumption that the material flows in the same way as a gas under extreme conditions belies the basic nature of an elastic solid. Velocity profiles obtained from ramp compression experiments (e.g. Figure 1(b)) suggest the existence of both small amplitude elastic waves and plastic waves of larger amplitude. The former propagate through the material as the stress increases toward the yield stress, and the latter as the material is compressed further beyond the yield surface. Therefore, a proper account of violent elastic-plastic deformation must account for a combination of large plastic deformation and the small deformations due to the inherent elasticity of the material.

In this paper we present a mathematical model for violent elastic-plastic deformation in the regime where the applied stress greatly exceeds the yield stress of the material. As we shall see, a distinguishing feature of our formulation is that in the limit of zero yield stress the model reduces to the equations of barotropic flow, while the effects of strength are treated as small perturbations to this leading order model. We will then present numerical solutions of our model, which are intended to simulate the experimental conditions of ICEs. This analysis will show that the inclusion of elastic effects gives rise to significant features of the material response which cannot be resolved by a barotropic flow model alone.

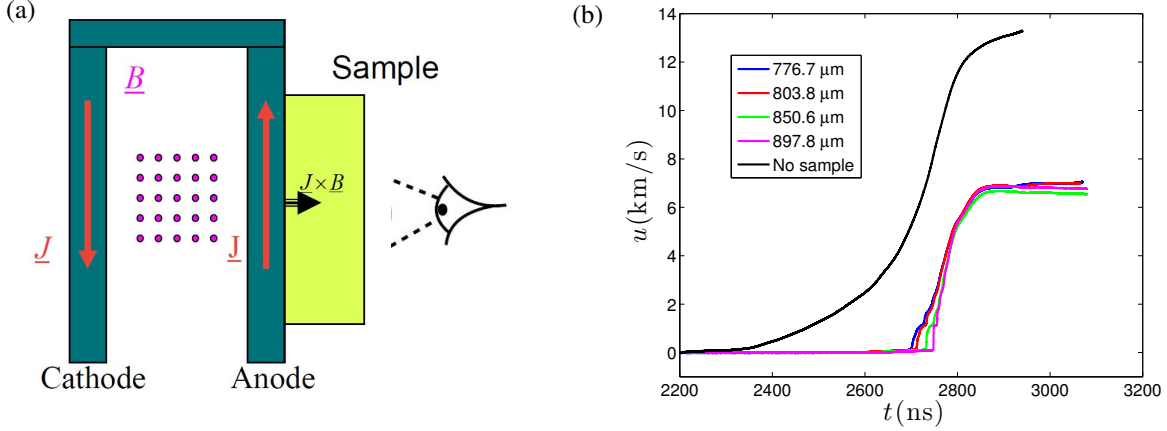


FIGURE 1: (a) Schematic of a ramp compression experiment. A baseplate plate is driven against a target plate in such a way that shocks are not allowed to form. Typical peak pressures are on the order of 10^2 GPa while the yield stress can be as low as 10^{-1} GPa (b) Experimental data obtained from the 3MBar compression of lead [1].

MATHEMATICAL MODEL

In this Section we derive a one-dimensional elastoplastic model in the regime where the applied stress is far in excess of the yield stress. It is traditional in problems of solid mechanics to operate in a Lagrangian framework, hence we will consider the situation in which a material element initially at Lagrangian position (X, Y, Z) is displaced to the Eulerian position $(x(X, t), Y, Z)$ after time t .

Governing equations

We begin by defining the relative specific volume $v = \rho_0/\rho = \partial x/\partial X$ and the axial velocity $u = \partial x/\partial t$, where ρ is the density and ρ_0 is the initial density which is assumed to be constant. These two quantities are related by the kinematic equation

$$\frac{\partial v}{\partial t} - \frac{\partial u}{\partial X} = 0. \quad (1)$$

The total deformation gradient F is assumed to be purely one-dimensional and is obtained by a multiplicative decomposition into an elastic and plastic part

$$F = \text{diag}(v, 1, 1) = F^e F^p, \quad (2)$$

where the elastic and plastic deformations are each assumed to be uniaxial:

$$F^e = \text{diag}(F_1^e, F_2^e, F_2^e), \quad F^p = \text{diag}(F_1^p, F_2^p, F_2^p). \quad (3)$$

Hence we obtain the relations

$$F_1^e F_1^p = v, \quad F_2^e F_2^p = 1. \quad (4)$$

Since we are considering uniaxial deformation the stress tensor is diagonal, and conservation of momentum implies that

$$\rho_0 \frac{\partial u}{\partial t} = \frac{\partial \sigma_1}{\partial X}, \quad (5)$$

where σ_1 is the axial stress.

In the absence of heat sources and thermal conduction, the equation for conservation of energy reads

$$\frac{\partial}{\partial t} \left(\frac{1}{2} \rho_0 u^2 + \mathcal{W} \right) = \frac{\partial}{\partial X} (u \sigma_1), \quad (6)$$

where \mathcal{W} is the internal energy per unit reference volume. By expanding out (6), and using (1) and (5), we can alternatively write

$$\frac{\partial \mathcal{W}}{\partial t} = \sigma_1 \frac{\partial v}{\partial t}. \quad (7)$$

We now suppose that \mathcal{W} is a function of the elastic deformation components F_1^e and F_2^e and the entropy S . The stress components and the temperature T are then derivable from \mathcal{W} using

$$T = \frac{1}{\rho_0} \frac{\partial \mathcal{W}}{\partial S}, \quad \sigma_1 = \frac{1}{\nu} F_1^e \frac{\partial \mathcal{W}}{\partial F_1^e}, \quad \sigma_2 = \frac{1}{\nu} \frac{F_2^e}{2} \frac{\partial \mathcal{W}}{\partial F_2^e}, \quad (8)$$

where the factor of 2 in the expression for σ_2 arises from the uniaxiality assumption. Later we will specialise the form of \mathcal{W} to one suitable to problems of large plastic deformation. Using the relations (8) we can write the energy equation (7) in the form

$$\rho_0 T \frac{\partial S}{\partial t} = \frac{2\nu(\sigma_1 - \sigma_2)}{F_2^e} \frac{\partial F_2^e}{\partial t}. \quad (9)$$

To close the model, we specify a flow rule for the irreversible plastic flow which occurs when the stress in the material reaches and exceeds the yield stress. Following Howell et al. [2], we define the associated flow rule

$$\frac{1}{F_1^p} \frac{\partial F_1^p}{\partial t} = -\frac{2}{F_2^p} \frac{\partial F_2^p}{\partial t} = \Lambda \frac{\partial f}{\partial \sigma_1} \quad (10)$$

where Λ is the flow rate. Note that a first integral of these equations yields the relation

$$F_1^p F_2^{p2} = 1. \quad (11)$$

Thus the plastic deformation is incompressible. The restriction that the flow rate $\Lambda \geq 0$ also precludes the possibility of negative dissipation.

The simplest model of plasticity is that of rate-independent perfect plasticity, in which the stress cannot exceed the yield stress. This leads to a yield criterion of the form

$$f(\sigma_1, \sigma_2) \leq \sigma_Y, \quad (12)$$

where $f(\sigma_1, \sigma_2)$ is called the yield function. In what follows we use the Tresca yield function

$$f(\sigma_1, \sigma_2) = |\sigma_1 - \sigma_2|. \quad (13)$$

However, in violent impact experiments the stress may be far in excess of the yield stress and hence (12) no longer holds. Instead, we expect the plastic flow rate Λ to be an increasing function of the amount by which the deviatoric stress exceeds the yield stress which leads us to define

$$\Lambda = r \left[\frac{|\sigma_1 - \sigma_2|}{\sigma_Y} - 1 \right]^+ \quad (14)$$

where

$$[x]^+ = \begin{cases} 0 & \text{if } x \leq 0 \\ x & \text{if } x > 0 \end{cases} \quad (15)$$

and r is a rate constant with units of inverse time. A rate-independent plasticity model is recovered in the limit $r \rightarrow \infty$. Using Equation (14), the flow rule (10) becomes

$$\frac{1}{F_1^p} \frac{\partial F_1^p}{\partial t} = rG \left(\frac{\sigma_1 - \sigma_2}{\sigma_Y} \right) \quad (16)$$

where

$$G(z) = z + \frac{1}{2}|z - 1| - \frac{1}{2}|z + 1| \quad (17)$$

as shown in Figure 2.

In summary, once we have specified an equation of state \mathcal{W} , Equations (1), (4), (5), (8), (9), (11), and (16) provide a closed system of nine equations for the nine unknowns ν , u , S , F_1^e , F_2^e , F_1^p , F_2^p , σ_1 , and σ_2 .

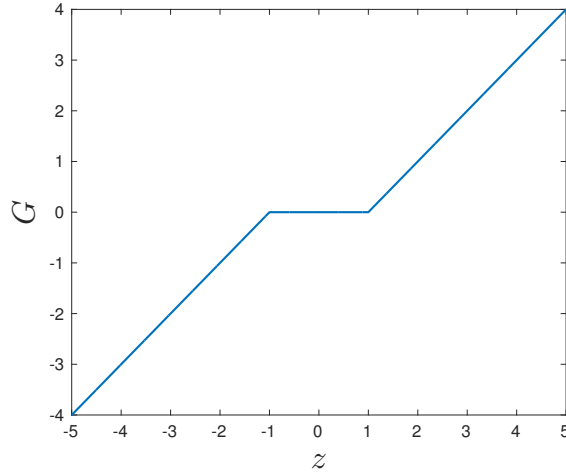


FIGURE 2: Plot of the yield function G

Equation of state

To close our model, we must specify a constitutive equation for the strain energy density \mathcal{W} . We are interested in the regime where a material undergoes large plastic deformation with $O(1)$ variations in density. Inspection of Equations (1) and (5) suggests that the axial stress must then be $O(\rho_0 c_0^2)$ where c_0 represents a typical sound speed. However, turning to the yield condition (13) we observe that the deviatoric stress $\sigma_1 - \sigma_2$ must be of the same order as the yield stress σ_Y which is typically much smaller than the axial stress. We conclude therefore that, although the volumetric part of the deformation may undergo $O(1)$ variations, the deviatoric elastic strain will be much smaller of order $\delta = \sigma_Y / \rho_0 c_0^2 \ll 1$. It is therefore useful to define

$$F_1^e = \nu^{\frac{1}{3}} \sqrt{1 + 2\delta\varepsilon}, \quad F_2^e = \frac{\nu^{\frac{1}{3}}}{(1 + 2\delta\varepsilon)^{\frac{1}{4}}} \quad (18)$$

where $\delta\varepsilon$ is a measure of the deviatoric elastic strain.

By exploiting the smallness of δ , we can expand \mathcal{W} in a Taylor series:

$$\frac{\mathcal{W}}{\rho_0 c_0^2} \sim \mathcal{W}_0(\nu, S) + \delta^2 \mathcal{W}_2(\nu, S) \varepsilon^2 + O(\delta^3), \quad (19)$$

noting that $\varepsilon = 0$ is a local minimum of the elastic energy. The term \mathcal{W}_0 is the leading order, thermodynamic part of the equation of state, while \mathcal{W}_2 is analogous to the shear modulus of the material.

From Equation (9) we now infer that, in the absence of shocks, the entropy production through dissipation is small so that

$$S = S_0(1 + \delta s) \quad (20)$$

where $s = O(1)$ and the initial entropy S_0 is assumed to be constant. We can therefore restrict Equation (19) further to

$$\frac{\mathcal{W}}{\rho_0 c_0^2} \sim h(\nu) + \delta s \theta(\nu) + \delta^2 \left(s^2 S_0^2 \frac{\partial^2 \mathcal{W}_0}{\partial S^2}(S_0, \nu) + \frac{1}{2} k(\nu) \varepsilon^2 \right) + O(\delta^3), \quad (21)$$

where $h(\nu) = \mathcal{W}_0(S_0, \nu)$, $\theta(\nu) = S_0 \frac{\partial \mathcal{W}_0}{\partial S}(S_0, \nu)$ and $k(\nu) = 2\mathcal{W}_2(S_0, \nu)$ are in principle known functions.

Finally, we find the following approximations for the stress components

$$\frac{\sigma_1}{\rho_0 c_0^2} \sim h'(\nu) + \delta \left(s \theta'(\nu) + \frac{2k(\nu)}{3\nu} \varepsilon \right) + O(\delta^2), \quad \frac{\sigma_1 - \sigma_2}{\sigma_{Y0}} \sim \frac{k(\nu)}{\nu} \varepsilon + O(\delta). \quad (22)$$

Non-dimensionalisation

We non-dimensionalise the governing equations as follows

$$X = L\tilde{X}, \quad t = \frac{L}{c_0}\tilde{t}, \quad u = c_0\tilde{u}, \quad (23)$$

where L is a typical sample length. In dimensionless form, the governing equations (1), (5), (9) and (16) in the limit $\delta \rightarrow 0$ reduce to

$$\frac{\partial v}{\partial t} - \frac{\partial u}{\partial X} = 0, \quad (24)$$

$$\frac{\partial u}{\partial t} - h''(v)\frac{\partial v}{\partial X} = 0, \quad (25)$$

$$\theta(v)\frac{\partial s}{\partial t} = \frac{2k(v)\varepsilon}{3v}\frac{\partial v}{\partial t}, \quad (26)$$

$$\frac{2a}{3v}\frac{\partial v}{\partial t} = G\left(\frac{\varepsilon}{\varepsilon_c(v)}\right), \quad (27)$$

where

$$\varepsilon_c(v) = \frac{\sigma_Y(v)v}{\sigma_{Y0}k(v)} \quad (28)$$

represents the normalized yield strain, and

$$a = \frac{c_0}{rL} \quad (29)$$

is a dimensionless rate constant.

The salient feature of the leading-order model outlined above is that Equations (24) and (25) constitute a model for barotropic flow with an equation of state $h(v)$. Note that the energy equation and the plastic flow rule decouple at this order, hence s and ε may be determined *a posteriori* from (26) and (27). However, owing to the nature of the function G we note that Equation (27) is degenerate when the left-hand side is identically zero. This suggests the existence of a distinguished asymptotic limit when $\partial v/\partial t$ is small. We investigate this limit by considering small perturbations to the governing equations close to equilibrium.

Small amplitude oscillations

To examine the behaviour of the governing equations when the displacement is small, we perform the re-scalings

$$v = 1 + \delta\eta, \quad u = \delta U, \quad s = \delta\zeta \quad (30)$$

before taking limit $\delta \rightarrow 0$. The leading order governing equations in this case are

$$\frac{\partial \eta}{\partial t} - \frac{\partial U}{\partial X} = 0, \quad (31)$$

$$\frac{\partial U}{\partial t} - \frac{\partial \eta}{\partial X} - \frac{2k_0}{3}\frac{\partial \varepsilon}{\partial X} = 0, \quad (32)$$

$$\theta(1)\frac{\partial \zeta}{\partial t} = k_0\varepsilon\left(\frac{2}{3}\frac{\partial \eta}{\partial t} - \frac{\partial \varepsilon}{\partial t}\right), \quad (33)$$

$$a\delta\left(\frac{2}{3}\frac{\partial \eta}{\partial t} - \frac{\partial \varepsilon}{\partial t}\right) = G(\varepsilon). \quad (34)$$

where $k_0 = k(1)$, and we assume $h''(1) = \varepsilon_c(1) = 1$ by the choice of scalings c_0 and σ_{Y0} . If $a\delta = O(1)$, Equations (31), (32) and (34) provide a coupled semi-linear hyperbolic system for η , v and ε , while the entropy change $\delta^2\zeta$ is again negligible to lowest order and may be determined *a posteriori* from Equation (33).

All of the preceding analysis suggests that entropy variations are universally negligible in the absence of shocks and a uniformly valid model which captures all of the above behaviour is

$$\frac{\partial v}{\partial t} - \frac{\partial u}{\partial X} = 0, \quad (35)$$

$$\frac{\partial u}{\partial t} - \frac{\partial}{\partial X} \left(h'(\nu) + \frac{2\delta k(\nu)}{3\nu} \varepsilon \right) = 0, \quad (36)$$

$$a \left(\frac{2}{3\nu} \frac{\partial \nu}{\partial t} - \delta \frac{\partial \varepsilon}{\partial t} \right) = G \left(\frac{\varepsilon}{\varepsilon_c(\nu)} \right). \quad (37)$$

In regions where the strain is $O(1)$, terms involving the small parameter δ are negligible, and we retrieve the leading-order equations of barotropic flow. However, in regions where the strain is $O(\delta)$, the deviatoric and isotropic contributions to the strain balance, and hence we expect that effects of elasticity will be noticeable near the tails of propagating waves.

NUMERICAL SOLUTIONS

We now study the predictions of our model for the elastic and plastic waves that propagate through a metal sample when subjected to a compressive force at $X = 0$. The governing partial differential equations (35)–(37) are of hyperbolic type, so we use the method of Kurganov and Tadmor [3] to compute numerical solutions.

The simplest initial and boundary conditions that we can impose to simulate violent compression are

$$\nu = 1, \quad u = 0, \quad \varepsilon = 0 \quad \text{at} \quad t = 0, \quad X > 0, \quad (38)$$

$$u = U_0(t) \quad \text{at} \quad X = 0, \quad t > 0. \quad (39)$$

For simplicity, and to compare with a leading order barotropic flow model that resembles homentropic gas dynamics, we make the following constitutive assumptions:

$$h(\nu) = \frac{1}{\gamma(\gamma - 1)\nu^{\gamma-1}}, \quad k(\nu) = K = \text{constant}, \quad \varepsilon_c(\nu) = 1 \quad (40)$$

where $K > 0$ and $\gamma > 1$ are constants.

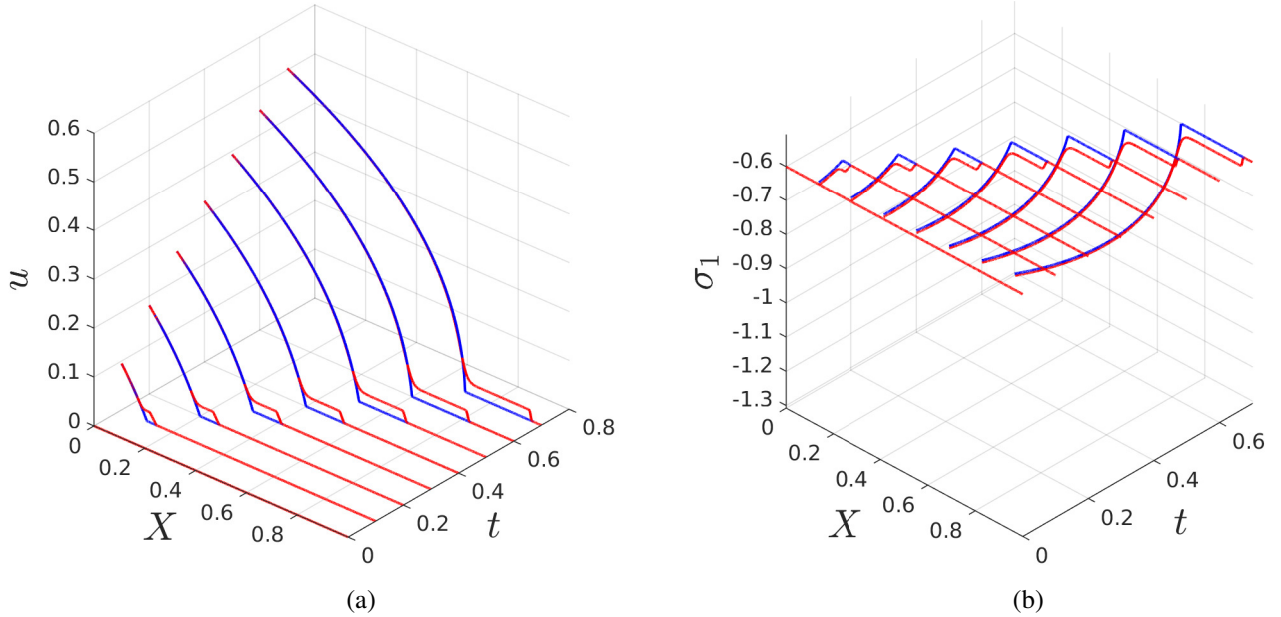


FIGURE 3: Numerical solutions of the problem (35)–(39) in red for (a) the velocity, u , and (b) the axial stress, σ_1 , plotted versus the Lagrangian position X at times $t = 0, 0.1, \dots, 0.7$. The parameter values used were $U_0 = 1$, $\gamma = 5/3$, $K = 2$, $a = 0.1$, $\delta = 0.01$. The blues curves show the corresponding results for the barotropic flow model when $\delta = 0$.

Figure 3 shows numerical solutions of the problem (35)–(39) for (a) the velocity $u(X, t)$, and (b) the axial stress

$$\sigma_1 = h'(\nu) + \frac{2\delta k(\nu)}{3\nu} \varepsilon. \quad (41)$$

The solutions for our elastic-plastic model are shown in red, while those for the barotropic flow model ($\delta = 0$) are in blue. We observe that initially the two models are essentially indistinguishable except that the elastic-plastic model exhibits a faster moving elastic precursor which propagates ahead of a much larger plastic wave into undisturbed material. This confirms our expectation that elastic effects should be most prominent in regions where the strain is small. Between the rear of the elastic wave and the front of the plastic wave exists a “plateau” region where $\varepsilon \approx -1$ and the material remains close to the yield surface.

The quantity which can be measured in ICEs is the velocity of the stress-free surface of the target material. To study this phenomenon, we introduce the additional boundary condition $\sigma_1(1, t) = 0$. Figure 4(a) plots a comparison of the free-surface velocity of the two competing models. Focusing on the elastoplastic model, plotted in red, we see that the first arrival at the free surface is that of the elastic precursor, resulting in a small rise in velocity. This is followed by a period of constant velocity since the plastic wave speed is initially less than that of the elastic wave speed. We then observe a staircase-like feature, with the velocity increasing in a series of small steps. This persists until the large amplitude plastic wave arrives at the free-surface, at which point there is a rapid increase in the velocity. In comparison, the barotropic flow model retains only the feature of the rapid increase in velocity caused by the bulk wave arriving at the free surface.

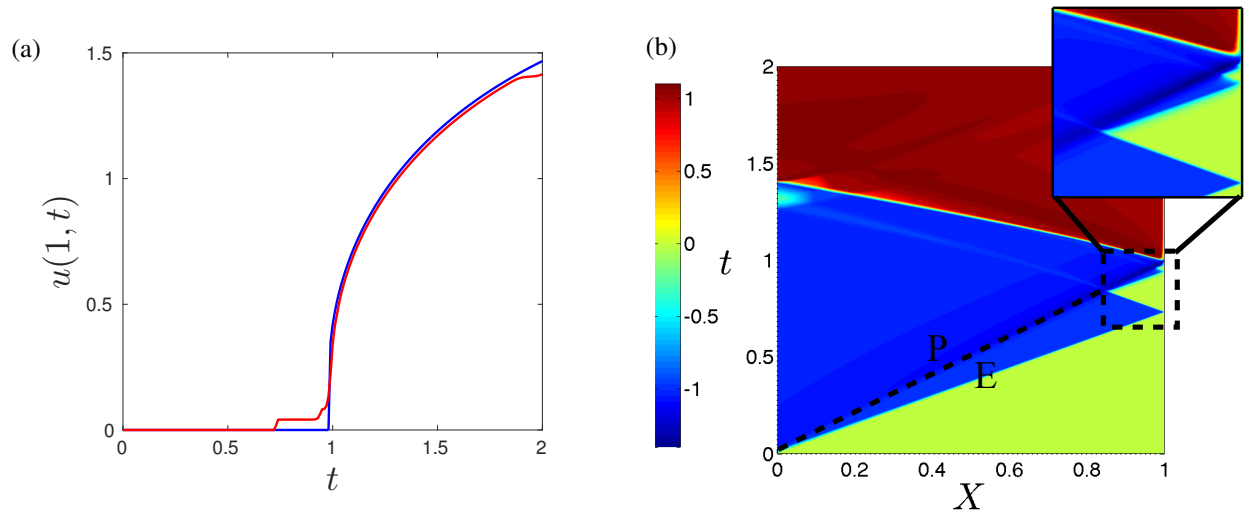


FIGURE 4: (a) Free-surface velocity $u(1, t)$ computed using the elastoplastic model (35)–(39) (red). The corresponding barotropic flow solution ($\delta = 0$) is shown in blue. (b) Numerical solution of the model (35)–(39) for the deviatoric strain $\varepsilon(X, t)$ using the same parameter values as in Figure 3.

The aforementioned observations may be explained by studying the dynamics of the elastic waves over the time-scale of the experiment. In Figure 4(b) we plot a heat map of the deviatoric strain $\varepsilon(X, t)$. Regions where the material is undisturbed are characterised by $\varepsilon = 0$, elastic regions by $|\varepsilon| \leq 1$ and the material is plastic wherever $|\varepsilon| > 1$. Initially an elastic wave labelled E propagates ahead of a much larger plastic wave P, eventually reflecting off the free-surface and back toward the incoming plastic wave. As the two waves interact (see inset), part of the elastic wave is transmitted through the plastic wave and part is transmitted back toward the free-surface which explains the second small increase in velocity observed in Figure 4(a). The elastic wave therefore reverberates back and forth until the arrival of the much larger plastic wave. Furthermore, this reverberation appears to result in a degradation of the plastic wave, which attains a lower final surface velocity at $t = 2$ in comparison to the model based on barotropic flow.

CONCLUSIONS

We have presented a mathematical model for the violent uniaxial deformation of a metal sample in the regime where the ratio of the yield stress to the applied stress is small. This ratio is manifested in the non-dimensional parameter δ . In the limit of zero yield stress, i.e. $\delta \rightarrow 0$, the model reproduces the hydrodynamic models currently used in the analysis of isentropic compression experiments, while the effects of elasticity are small perturbations to this leading order model. This is advantageous as it allows a direct comparison to be made between the two models.

To analyse the elastoplasticity model, we considered the problem of uniaxial ramp compression of a metal target. The solutions of this problem were computed numerically in the first instance. These solutions reveal the presence of

both large amplitude plastic waves and elastic waves of smaller amplitude. The deviation from gas dynamics caused by the inclusion of elasticity can be further appreciated by considering the velocity at the stress-free boundary of the target material. The most striking observation is the reflection of elastic waves from the free surface, which can result in degradation of the incoming plastic wave and also may lead to a cumulative $O(1)$ increase in the free surface velocity prior to the arrival of the plastic wave. This observation is significant since the elastic waves, although considered a small perturbation to the gas dynamics model, may lead to appreciable differences in the velocity trace used in an inverse analysis to determine the EoS of a material.

The evidence provided by the numerical solutions presented in this paper give rise to a number of interesting mathematical questions. In particular, using a mixture of asymptotic and numerical techniques we suggest that it is possible to track the progress of the elastic waves through the sample as the experiment proceeds. This appears to be an important step in approaching the inverse problem of obtaining equation of state information of a highly plasticised material in the presence of shear strength.

ACKNOWLEDGMENTS

The authors would like to thank Dr. C. Robinson and Dr. J. Turner for many helpful and insightful discussions during this project. This work was jointly funded by EPSRC and AWE plc under the grant number EP/I501592/1.

REFERENCES

- [1] S. Rothman, J.-P. Davis, M. Knudson, T. Ao, and S. Gooding, *Bulletin of the American Physical Society* **58** (2013).
- [2] P. D. Howell, G. Kozyreff, and J. R. Ockendon, *Applied solid mechanics*, 43 (Cambridge University Press, 2009).
- [3] A. Kurganov and E. Tadmor, *Journal of Computational Physics* **160**, 241–282 (2000).
- [4] P. D. Howell, H. Ockendon, and J. R. Ockendon, “Mathematical modelling of elastoplasticity at high stress,” in *Proceedings of the Royal Society of London A: Mathematical, Physical and Engineering Sciences* (The Royal Society, 2012).